# Future Sustainability

**Open Access Journal** 

ISSN 2995-0473

Journal homepage: https://fupubco.com/fusus

Future Publishing LLC

https://doi.org/10.55670/fpll.fusus.2.1.2

Review

# The extraction process of nanocellulose from organic waste and incorporating it into biopolymers for mechanical property enhancement

# Lamia Afrin Ratry, Md Bazlul Mobin Siddique\*

Faculty of Engineering Computing and Sciences, Swinburne University of Technology Sarawak Campus, Jalan Simpang Tiga, Sarawak, Malaysia

## ARTICLE INFO

# Article history: Received 20 September 2023 Received in revised form 24 October 2023 Accepted 5 November 2023

### Keywords:

Nanocellulose, Organic waste, Biopolymers, Hydrolysis, Chemical extraction

\*Corresponding author Email address: msiddique@swinburne.edu.my

DOI: 10.55670/fpll.fusus.2.1.2

### ABSTRACT

Nanocellulose possesses excellent properties such as an elastic modulus of 220 GPa, Young's modulus of 10-150 GPa, low density of around 1.6 g/cm<sup>3</sup>, and high thermal stability. To enhance mechanical flexibility, nanocellulose can strengthen the bio-polymers. This research project aims to review the extraction methods and the characterization of the nanocellulose extracted from organic waste materials such as banana peel, pineapple leaf fiber, crown, corncob, palm oil, etc., focusing on the possibility of adding the nanocellulose to enhance the properties such as tensile strength, young's modulus, water vapor permeability of the biopolymers. Chemical extraction methods like alkaline treatment, bleaching treatment, sulfuric and formic acid hydrolysis, TEMPOmediated oxidation, and mechanical extraction methods such as ball milling, ultrasonication, high-pressure homogenization, and grinding have been studied. The results obtained from all the characterization techniques have been tabulated. From the results tabulation, the length of cellulose nanocrystal and cellulose nanofiber is 100-350 nm and 350 nm and above, respectively. The hydrolysis time and the types of acid used will affect the yield and aspect ratio; the acid concentration will also affect the degradation temperature. Mechanical treatment results in a higher yield of the nanocellulose, but mechanical treatment is not economically solvent due to the heavy use of power. Considering that nanocellulose extracted via chemo-mechanical treatment has outstanding characteristics that can potentially improve the mechanical properties when incorporated into the biopolymers.

### 1. Introduction

In the past decades, the rate of environmental pollution has increased manifold. The world is largely dependent on synthetic products, and the excess use of synthetic polymer products has caused harmful effects on the environment, such as global warming and plastic waste. It is an urgent need to solve the environmental crisis the world is facing today and find safer, greener, environmentally friendly solutions. Hence, continuous research is ongoing to develop sustainable products that eventually eliminate fossil fuel dependence. One of the concepts' recently getting attention is bio-based

products reinforced with nanocellulose because of their biodegradability and eco-friendly. The incorporation of nanofillers into polymers allows the production of high-mechanical-performance composites [1]. Since biopolymers have low mechanical properties relative to conventional polymers, their applications have been restricted to commodity materials. To enhance mechanical flexibility, researchers looked for ways to reinforce nanomaterials without losing the environmental benefits of biopolymers [2]. As an abundant and biobased material, nanocellulose can be prepared from various plant biomass, bacteria, algae, and

marine invertebrate animals (tunicates) using different methods [3]. This project focuses on reviewing the extraction methods of nanocellulose from organic waste materials. Billions of tons of organic waste are generated, and fruit and vegetable peels are the highest. In 2019, 17 % of the global food production was wasted, accounting for 931 million tons. The wastes are either buried or dumped in landfills, but they can be sold as value-added products if they are reused. Agricultural waste fibers have a lot of potential in composites because of their high strength, environmental friendliness, low cost, and availability. That is why they are a remarkable resource for nanocellulose extraction [3]. Banana peel contains a significant amount of cellulose (12%). This content may be used as a reinforcement ingredient in highperformance composite films [4]; pineapple leaf fibers are mostly made up of cellulose (81.27%), corn contains about 35-50 % cellulose [5], potato contains 30-40 % of cellulose. Greater extractive and lignin concentration lowers nanocellulose extraction yield and increases chemical and energy usage during removal, resulting in higher costs [6]. The research project aims to review different methodologies for the feasible extraction of nanocellulose from the cellulose part of the organic waste and its characterization to test its suitability as a composite to enhance the biopolymers' mechanical properties.

### 2. Methodology

### 2.1 Materials

All the information was gathered from published literature on the scientific platform and was available through the university library network. The data was checked, and numerical values were tabled to compare the products and their characteristics.

### 2.2 Percentage of Yield

After the extraction, the yield of the nanocellulose will be determined. The yield can be calculated from the difference between the initial bran mass and the final bran mass (on a dry basis) of the bran. The formula is given below:

Yield (%) = 
$$\frac{g \text{ of nanofiber (db)}}{g \text{ of bran (db)}} \times 100$$
 (1)

### 2.3 Water vapor permeability (WVP)

Water vapor permeability is the material's ability to let water vapor, or any gas, penetrate inside. Water vapor permeability can be calculated as such:

$$WVP = \frac{w}{t} \times \frac{\delta}{A \cdot AP} \tag{2}$$

where: w/t is the slope of the line of weight gain (w) as a function of time (t) (g/s);  $\delta$  is the mean sample thickness (m); A is the sample permeation area (m²), and  $\Delta$ P is the difference in water vapor pressure through the sample for pure water at 25 °C (Pa) [4].

### 2.4 Thermal Gravimetric Analysis (TGA)

TGA is a form of thermal analysis that measures the mass of a sample against time or Temperature in a controlled setting. The sample can be analyzed in a crescent or at an isothermal temperature, with the Temperature falling at a steady rate [7]. Perkin Elmer's Diamond TG/DTA was used to examine the nanocellulose extracted from pineapple leaf samples' thermal properties. In a nitrogen atmosphere, about

10~mg of the sample was placed in the alumina cup and heated at a rate of  $20~^\circ\text{C/min}$  [8]. On the contrary, reference [9] used NETZSCH STA 449F3 (NETZSCH-Gerätebau GmbH, Germany) instrument.

### 2.5 Tensile Properties

The tensile properties tested for nanocellulose are Young's modulus, strain, and stress. Young's modulus is the ability to resist the change in length under the external force applied. Strain is the amount of deformation encountered when an external force is applied, whereas stress is the force acting on the unit area of the body. Reference [10] tested the tensile properties using an Instron 3345 K1669 universal testing machine with an Instron 10 N load cell (model 2519-101, serial number – 64560). Young's modulus (E), strain at break (E'), and stress at break ( $\sigma$ ') were calculated using the formula:

$$E = \frac{F}{A} \cdot \frac{l}{\Delta} = \frac{F}{\Pi \frac{d^2}{\Delta}} \cdot \frac{l}{\Delta} \tag{3}$$

$$\sigma' = \frac{P'}{A} = \frac{P'}{\Pi \frac{d^2}{4}} \tag{4}$$

$$\mathcal{E}' = \frac{\mathcal{E}}{I} \tag{5}$$

Where E was expressed in GPa,  $\sigma'$  in MPa and  $\epsilon'$  as a percentage value.

### 3. Discussion

### 3.1 Nanocellulose from various sources

To assess the effectivity of the processes involved, it is essential to investigate the morphology, composition, thermal and mechanical properties. Various characterization techniques like SEM, FTIR, XRD, TEM, stress-strain curve, and water-vapor permeability are used to assess the properties of the extracted nanocellulose. The results from these tests from various papers are tabulated in Table 1.

### 3.2 Morphology and composition

The removal of lignin, pectin, hemicellulose, and the behavior of these chemical components is critical, especially during nanocellulose separation. The successful removal of these non-cellulosic parts will impact the end value of the extracted nanocellulose. The type of alkali and bleaching agent used will determine the efficacy of removing the lignin, pectin, and hemicellulose part of the raw material. The chemicals attack lignin and hemicellulose before the main treatment is done completely. The changes can be observed in micrographs after the alkaline and bleaching treatment However, hydrolysis time does not affect the morphology because nano whiskers are somewhat impermeable to acid attack due to residual lignin that coats nano whiskers' surface. The hydrolysis durations employed did not impart any substantial morphological changes. FTIR analysis is used to determine cellulose polymorphs present in the extracted nanocellulose. The absorbance ratios of lignin (1510 cm<sup>-1</sup>) to cellulose (897 cm<sup>-1</sup>) as a factor of bleaching and hydrolysis time were computed to examine the influence of hydrolysis duration and bleaching on the elimination of lignin and cellulose [21]. The peaks determined by the FTIR analysis confirm the elimination of the non-cellulosic part.

Sources	Method of extraction	Length	Diameter	Yield	Aspect ratio	References
Banana peel,	Chemical combined with	360- above 500	7- 35 nm	5.1%, 8.9 %	13-50	[11-13]
Banana	high-pressure	nm				
pseudo-	homogenizer, TEMPO-					
stem,	mediated oxidation,					
Banana peel	Ultrasonication					
	combined with chemical					
	treatment					
Banana peel	Mechanical (Microwave,	180 - 2300 nm	70-90 nm	76.58 ± 1.97	12-16	[9]
	ball milling, and	Average – 1285		% (w/w)		
	ultrasonication)	nm				
Banana bract		240 – 2100 nm		74.47 ± 1.23		
		Average – 972		% (w/w)		
		nm				
Banana	Acid hydrolysis with	130-150 nm	7.2-10 nm	-	15.3- 24	[14, 15]
pseudo-	ultrasonication, Acid					
stem, sugar	(H <sub>2</sub> SO <sub>4</sub> hydrolysis)					
palm					_	
PALF,	Lime juice hydrolysis	100-420 nm	20-80 nm	-	High aspect	[8, 16]
Pineapple	with ball milling,				ratio, 6.3	
crown	Chemical (H <sub>2</sub> SO <sub>4</sub>					
	hydrolysis)					
PALF	Steam explosion	200-300 nm	32.5 nm	-	50	[17]
PALF	High-shear	88-1100 nm	40-70 nm	76.9 %	High aspect	[18]
	homogenization and				ratio	
	Ultrasonication					
Potato peel	Chemical (H2SO4	410 ± 181 nm	23 nm	41-42 %	41	[19]
	hydrolysis)					
Corn husk	Chemical (H2SO4	162 ± 35.9 nm	26.9 ± 3.35 nm	-	Least aspect	[20]
	hydrolysis)				ratio	
	Ultra-sonication method	Several hundred	20.14 ± 4.32	-	Wide range	]
		nanometer	nm			

In the FTIR analysis of banana pseudo stem as in Figure 1 and Figure 2, the peak in wavenumber 1731 cm<sup>-1</sup> for lignin, 1525 cm<sup>-1</sup> for aromatic ring vibrations, 1238 cm<sup>-1</sup> for guaiacyl ring breathing with C=O stretching, and 761  $cm^{\text{--}1}$  for C-H deformations was absent which proves the removal of the non-cellulosic part (Figure 3). As seen in Figure 4, peaks at wavenumbers around 3328  $cm^{\text{-}1}$  and 2900  $cm^{\text{-}1}$  are due to stretching vibration in hydroxyl (OH) and C-H groups, respectively. The aromatic ring resonance of lignin has a distinctive peak at wavenumber 1200–1300 cm<sup>-1</sup>. Due to the removal of lignin, after chemical and mechanical treatment, this peak vanished. On the other hand, reference [13] presented TEM images to confirm the presence of nanofibers, and SEM confirms the removal of lignin, pectin, and hemicellulose. The structure of CNC is highly crystalline and needle-like, and the structure of CNF is entangled and weblike, which supports better stability. After each chemical treatment, there are visible color changes in the samples. After consecutive alkaline and bleaching treatments, the sample becomes white or transparent in color. The parameters of hydrolysis determine the size of CNCs. The type of acid used will influence the appearance of the nanocellulose (Figure 5). Increased acidity, longer reaction times, and higher temperatures may result in smaller CNCs in general [22].

Most of the previous experiments performed have used strong acids like sulfuric acid and formic acid. Usually, 60-68 wt% of sulfuric acid is ideal for the desired yield of CNC. However, reference [8] used lime juice instead of sulfuric acid, and the results were similar to sulfuric acid hydrolysis. Lime juice successfully hydrolyzed the pineapple leaf fiber (Figure 6) to nanocrystalline structure, but it may be noted that lime juice might not be effective for other biomass sources. Acid hydrolysis produces smaller-length nanocellulose compared to the mechanical treatment process. For example, references [15, 16, 20, 24] used H<sub>2</sub>SO<sub>4</sub> hydrolysis, which resulted in the length in the range between 150-500 nm. It can be noticed that generally, the diameter range for acid hydrolysis is 7-35 nm, and for mechanical processes, it is 20-80 nm. However, sulfuric acid hydrolysis of coconut husk resulted in dimeters of 5-6 nm. This is because partial delignification has been done in the process, and the property of the coconut husk has also affected the length and diameter of the nanocellulose. To remove the acidic constituents, the sample must be washed many times with distilled water. Moreover, sulfuric acid is not environmentally friendly and is very harsh. To overcome these problems, a better methodology is TEMPO-mediated oxidation, and a higher yield can be achieved, too.

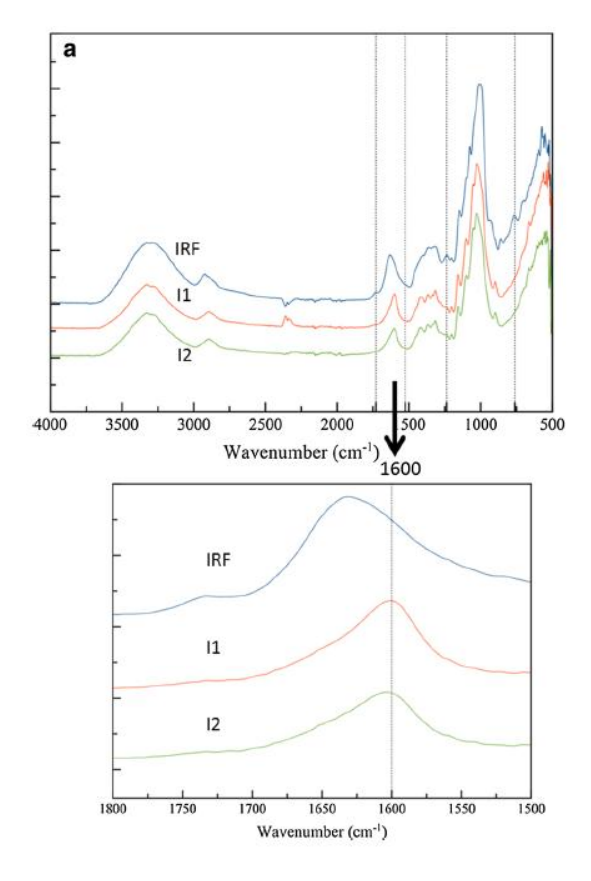


**Figure 1.** FTIR spectra of raw flour and nanocellulose from single and double bleaching from inner layer of stem [12]

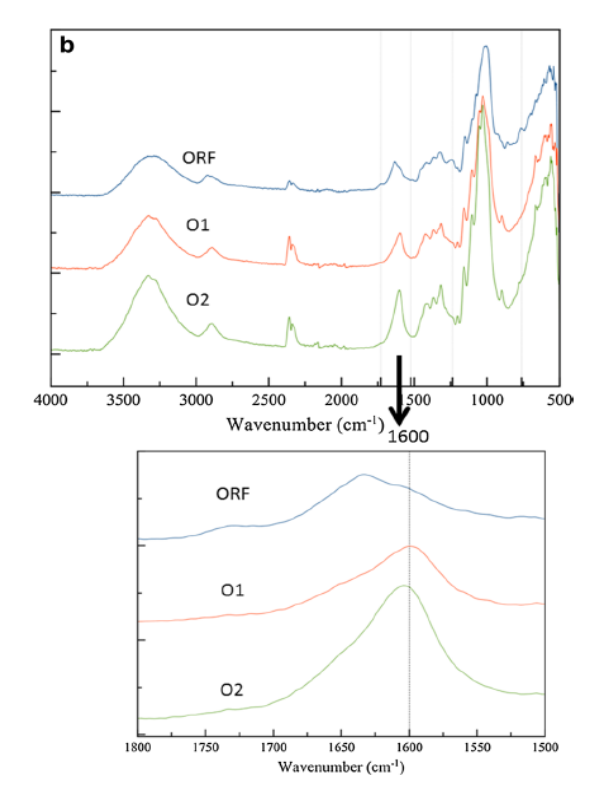


Figure 2. FTIR spectra of raw flour and nanocellulose from single and double bleaching from outer layer of stem [12]

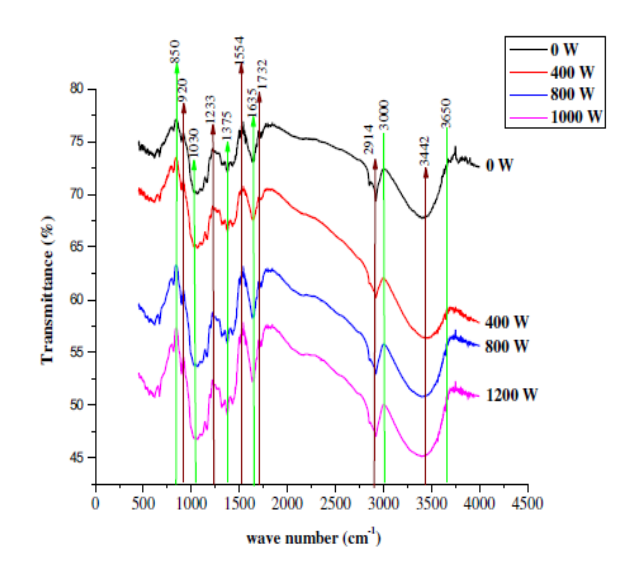


Figure 3. FTIR image of banana peel [13]

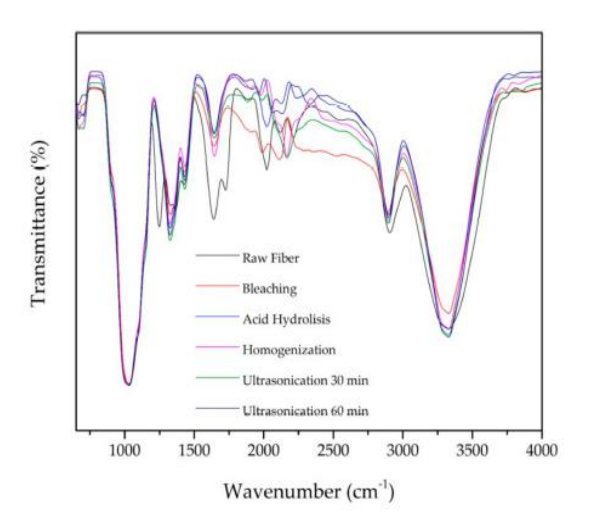
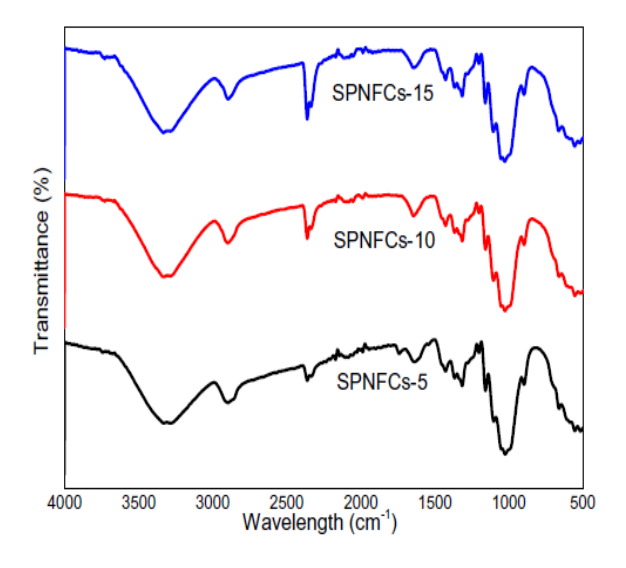


Figure 4. FTIR image of PALF [18]



**Figure 5.** FTIR image of sugar palm nanocellulose [15]

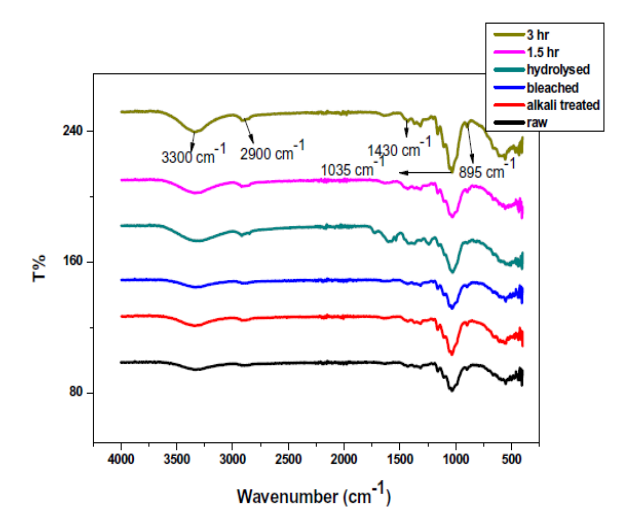


Figure 6. FTIR image of pineapple leaf [8]

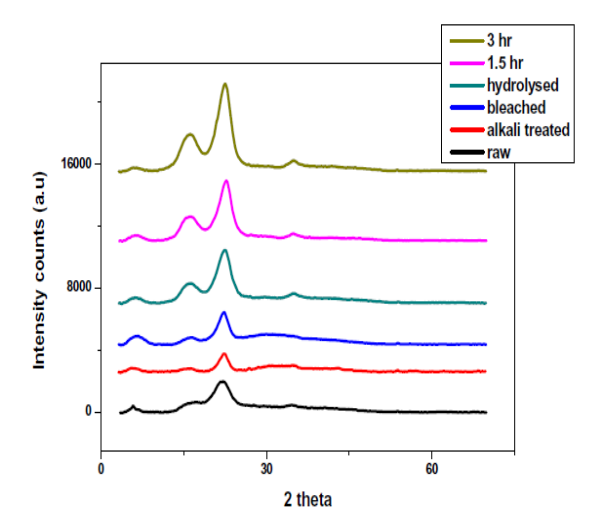
For example, corn cob [22], corn husk [24], and cotton husk [20] yielded more than 70% nitrocellulose when TEMPO-mediated oxidation was used as well as the aspect ratio was higher. For the effect of temperature and hydrolysis time it is relatively hard to understand the impact of temperature and hydrolysis time on the yield and aspect ratio for the impact of temperature and time. In general, with an increase in acid concentration, the hydrolysis time is decreased and vice versa. For corn cob [22], during sulfuric acid hydrolysis, 60 min was used at a temperature of 45 °C, and during formic acid hydrolysis, 30 min was used at a temperature of 95 °C. For 60 wt%, hydrolysis time was between 45-70 min at a temperature of 45-60 °C for banana, pineapple, and sugar palm biomass sources. Mechanical treatment yields the highest nanocellulose, particularly microwave treatment with ball milling and ultrasonication, and high-shear homogenization with ultrasonication yielded 74-78 % of nanocellulose fiber. Khawas and Deka [13] investigated the effect of different powers on the characteristics. CNFs were not evenly disseminated in water when the power output was 400 W. This improved noticeably when the power output was doubled to 800 W. With increasing ultrasonic power, the CNFs diffused significantly and produced a very dense suspension. Because of cavitation, high-intensity ultrasonic waves may create a very strong mechanical oscillation power. With the increased capacity, the length and the diameter decreased, resulting in a lower aspect ratio. However, mechanical treatment may not be economically feasible for large-scale applications due to the high consumption of mechanical treatment. Due to these drawbacks, chemical treatment followed by mechanical treatment is desirable. Nanocellulose extracted from banana peel and banana pseudo stem via chemo-mechanical and TEMPO-mediated oxidation resulted in a higher aspect ratio. In the case of cotton husk, a yield of 90-95 % was obtained. Nonetheless, mechanical treatment is not economical due to its high usage of power; moreover, to efficiently remove all the non-cellulosic parts, repeated cycles of mechanical treatment are required. Both chemical and mechanical treatment have drawbacks; considering all the effects of a combination of alkaline and bleaching pre-treatment, TEMPO-mediated oxidation and mechanical treatment can have better characteristics of nanocellulose to be used in polymers. Table 2 indicates the physical properties of nano cellulose extracted from various sources and using different methods.

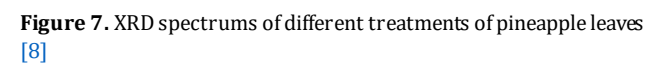
### 3.3 Crystallinity

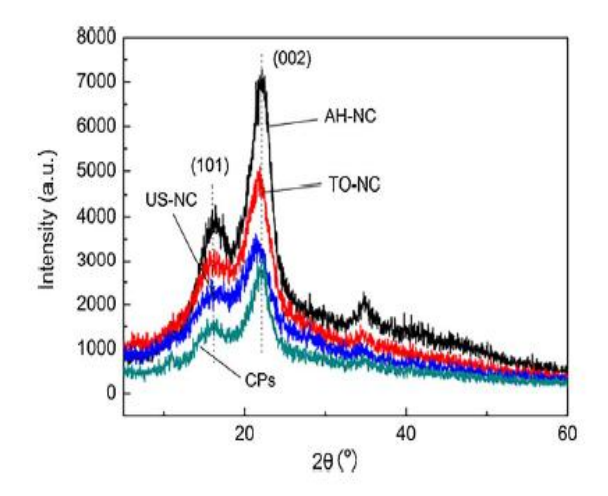
XRD analysis reveals the crystalline peak and index. Cellulose is partly crystalline and partly amorphous, which means that in the crystalline (ordered) portions of cellulose, mutual H-bonding will hold the cellulose chains together tightly. Still, in the amorphous (disordered) parts, weaker Hbonding will hold the cellulose chains together loosely [26]. Higher crystallinity can provide greater mechanical strength to the composite; hence, it is important to investigate. The crystalline peak 14-24 °C indicated the type I cellulose. Cellulose I polymorph is naturally found in the biomass, whereas cellulose I can be transformed into cellulose II polymorph after chemical modification. Crystalline peak is a means to confirm the polymorph orientation. Various factors like the source of nanocellulose, treatment process, type of acid, time of bleaching, and hydrolysis will affect both the CNC and CNF. However, there are no changes in the structure or composition of the crystal. Chemicals are more efficient in removing the amorphous region of the cellulose; hence, mechanical treatment with chemical pre-treatment results in high CRI. For example, nanocellulose from PALF [8] XRD curves presented in Figure 7, pineapple crown [14] and cornhusk [20] XRD curve presented in Figure 8; extracted via chemo-mechanical treatment resulted in CRI of 70-80 %. However, banana peel and banana bract [9] XRD exhibited high crystalline nanocellulose, which can be because of the repeated cycles of microwave pre-treatment to eradicate the non-cellulosic part. Similarly, the CI increased due to the increase of homogenization passages. After the treatments, the crystallinity of the bran sample increased by 300 percent, with the greatest value for sample N7 [11]. As seen in Figure 9, for 0, 400, 800, and 1000 W, the crystallinity index was 30.50, 44.14, 50.74, and 63.64 percent, respectively. The homogeneity and disintegration of the crystalline nature of CNFs were impacted by the output power level of high intensity ultrasonication, and crystallinity grew progressively as output power (1000 W) was raised [13]. In contrast, the typical peak of cellulose type I at 2=22.8° dropped substantially as the ball-milling duration increased, and the crystallinity index reduced by more than 50% when the milling time was longer than 2 hours. This could be due to the effect of mechanical energy on crystallinity. The strength of the acid will affect the crystallinity. For example, when formic acid was used in place of sulfuric acid for the extraction from corn cob [22], it resulted in a higher CRI. When formic acid was used, CRI rose to 63.8 percent, compared to 61.5 percent for corn cob residue crystallinity. Because formic acid was less hostile than sulfuric acid, it had a smaller impact on the crystalline area. The elimination of amorphous cellulose and non-crystalline lignin through formic acid hydrolysis resulted in greater crystallinity in comparison to those of amorphous cellulose and non-crystalline lignin (Figure 10 and Figure 11).

 $\textbf{Table 2.} \ Physical\ properties\ of\ the\ nano\ cellulose\ extracted\ from\ various\ sources\ and\ using\ different\ methods$ 

Sources	Method of extraction (treatment)	Degradation Temp	Diffraction Peak	Crystalline Index (XRD analysis)	References
Banana peel, PALF, Banana peel	Chemical combined with a high- pressure homogenizer, High-shear homogenization and Ultrasonication, Ultrasonication combined with chemical treatment	378- 381 °C, 220- 400 °C (Khawas & Deka 2016)	16°, 22°	44.14 % - 64.9 %	[11, 13, 18]
Banana peel (BP) Banana bract (BB)	Mechanical (Microwave, ball milling, and ultrasonication)	346 °C 214 °C	21°	77.2 % 75.8 %	[9]
Banana pseudo- stem	TEMPO-mediated oxidation	220 °C	15 °, 17.2 °, 22.2 °	57% - 70 %	[12]
PALF, Pineapple crown, sugar palm	Lime juice hydrolysis with ball milling, Chemical (H <sub>2</sub> SO <sub>4</sub> hydrolysis), Chemical with High-pressure homogenization	Maximum degradation temperature- 344 °C- 364 °C	15.8°, 22.5°	73 - 77 %	[8, 15, 16]
Corn cob	Sulfuric acid Formic acid TEMPO-mediated Pulp milling	313 °C 360 °C 305 °C	-	55.9 % 63.8 % 49.9 % 52.1 %	[22]
Corn husk	TEMPO-mediated oxidation  Ultra-sonication method  Chemical (H <sub>2</sub> SO <sub>4</sub> hydrolysis)	279 °C 348 °C 500 °C	16.26°, 22.63	72.33 % 53.47 % 83.51 %	[20]
Coconut husk	Chemical (H <sub>2</sub> SO <sub>4</sub> hydrolysis), TEMPO oxidation combined with sonication	Maximum 322 °C	15.6°, 22.7°, 34°	79- 83 %	[21]
Nypa Fruticans,		Maximum 207 °C			
Rice husk, Okara		Maximum 286 °C			
Coconut husk, shell	TEMPO-mediated oxidation	400°C	16.5 ° 22.5 °, 34.6 °	51-76 % (coconut shell), 56-73 % (coconut husk	[25]







 $\textbf{Figure 8.} \ \textbf{X-RD} \ patterns \ of nanocellulose \ samples \ of \ cornhusk \ \textbf{[20]}$ 

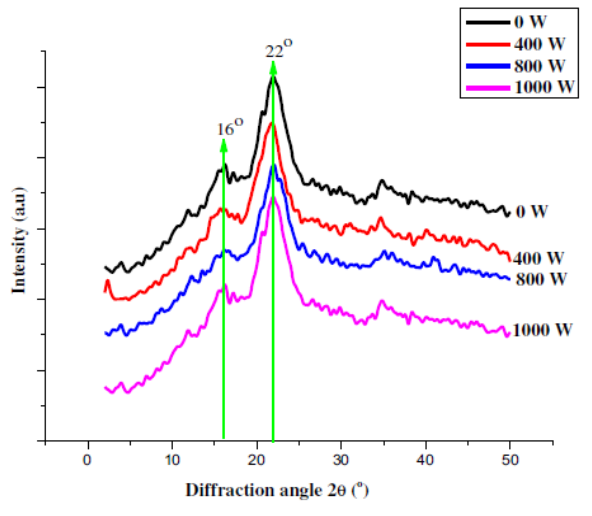


**Figure 9.** XRD diffraction pattern of cellulose nanofibers from culinary banana peel [13]

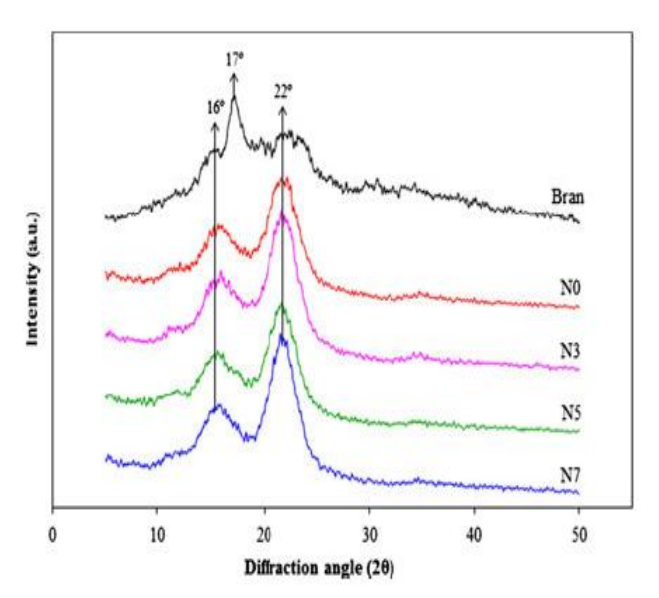
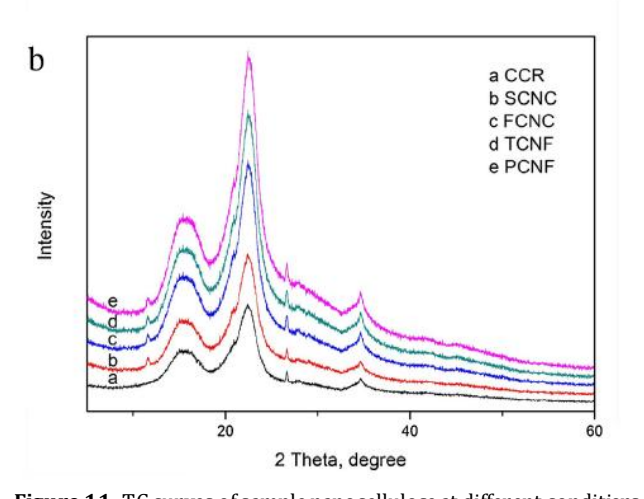


**Figure 10.** X-RD patterns of the banana peel bran and cellulose nanofibers obtained by different numbers of passages in the high-pressure homogenizer [11]



 $\textbf{Figure 11.} \ TG \ curves \ of sample \ nanocellulose \ at \ different \ conditions \ [22]$ 

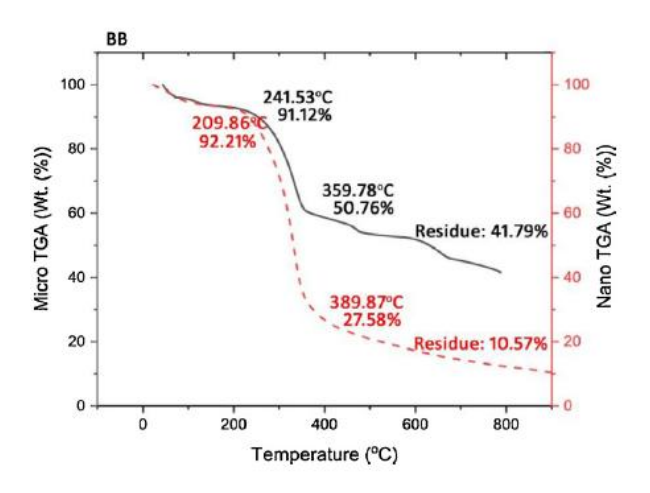


**Figure 12.** Thermogravimetric weight loss curves of micro and nano cellulose fibers of banana bract [9]

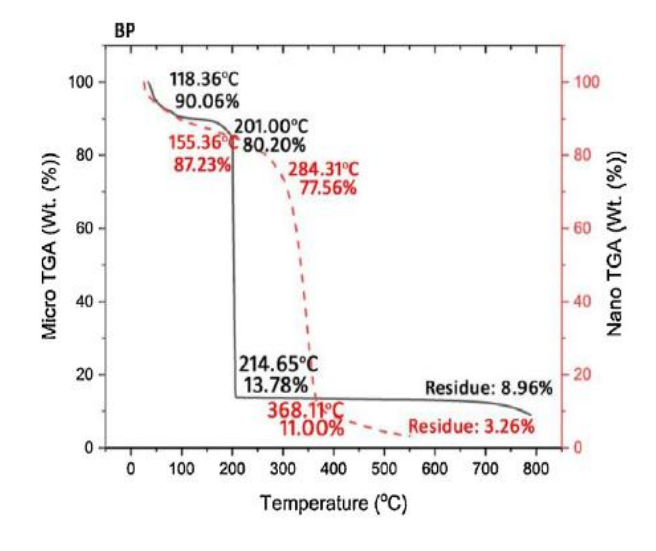


**Figure 13.** Thermogravimetric weight loss curves of micro and nano cellulose fibers of banana peel [9]

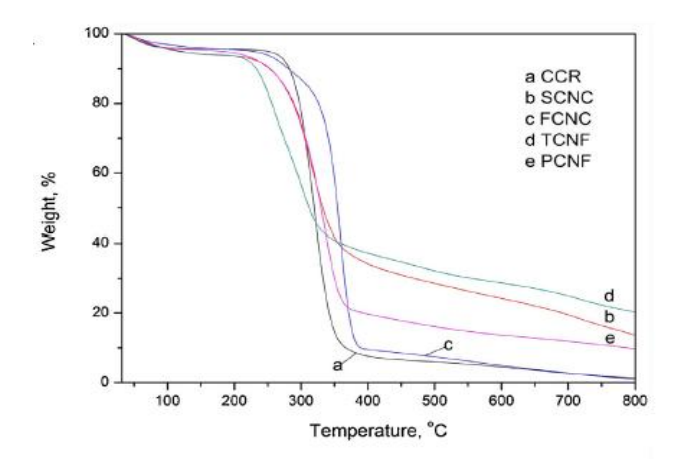


**Figure 14.** TG curve of nanocellulose samples extracted using a different methodology [22]

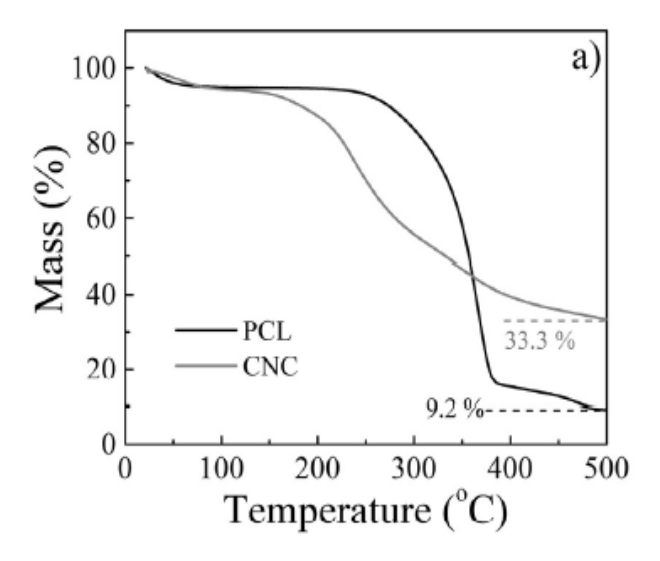


Figure 15. TG curves of pineapple crown [16]

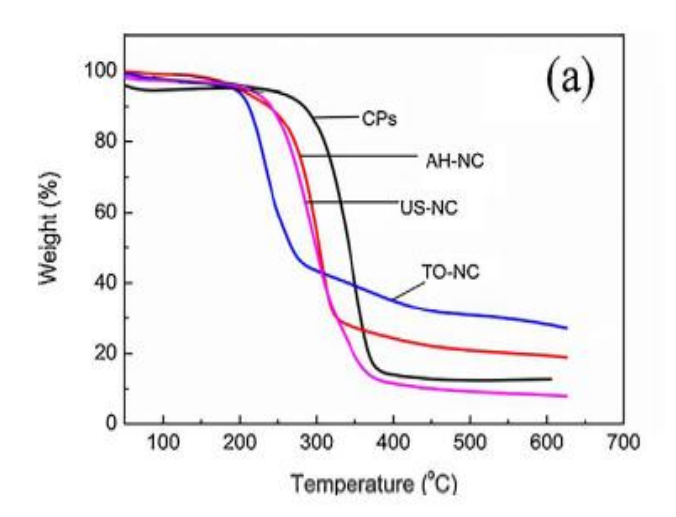
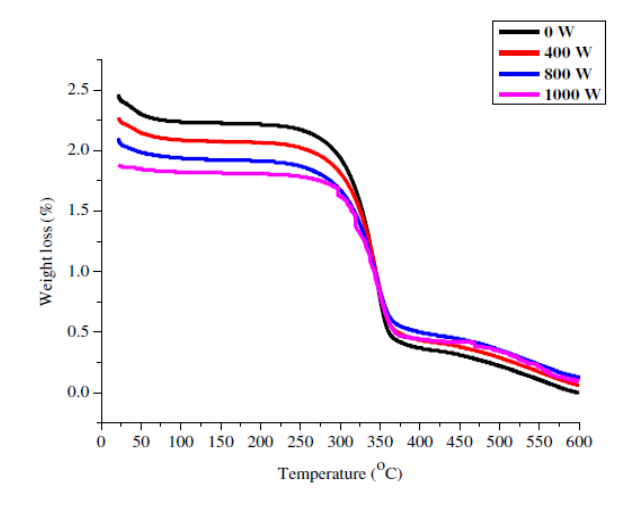


Figure 16. TG curve of corn fibers [20]



**Figure 17.** TG curve cellulose nanofibers from culinary banana peel [13]

### 3.4 Thermal properties

The early breakdown of hemicelluloses is followed by an early stage of pyrolysis of lignin, depolymerization of cellulose, active flame combustion, and char oxidation in lignocellulosic materials [27].

TGA curves reveal the degradation temperature gradient and help determine thermal stability at different temperatures. There is no observed trend in the thermal degradation of nanocellulose, but it is highly influenced by the source's structure and chemical composition. To a great extent, thermal stability is dependent on crystallinity. For example, PALF [8], pineapple crown [16], and sugar palm [15] had degradation temperatures above 320 °C when the crystallinity was more than 70%.

Similarly, nanocellulose extracted from corncob [22] via the formic acid analysis method had higher stability; this can be ascribed to the elimination of amorphous cellulose areas and residual lignin, its more significant degree of crystallinity. On the other hand, sulfuric acid significantly affects degradation temperature. A higher concentration of acids also lowers the degradation temperature due to the presence of the sulfate group. At 30 % v/v sulfuric acid concentration, there was no observed cellulose degradation, according to [28]. However, such a low acid concentration cannot remove lignin, pectin, and hemicellulose effectively, so a higher concentration of acid is used. According to reference [29], by adding sulfate groups due to sulfuric acid hydrolysis, the activation energies of cellulose nanocrystal degradation were considerably reduced. Moreover, surface sulfate groups are predicted to reduce the degradation temperature of CNF by either direct solid-to-gas phase transitions decarboxylation of surface carboxyl groups or indirect solidto-gas phase transitions from decarboxylation surface carboxyl groups [30]. The nanocellulose extracted via mechanical (Microwave, ball milling, and ultrasonication) treatment showed higher thermal stability. This can be due to the absence of alkaline and acid treatment. The temperature curves from banana peel and banana bract are shown in Figure 12 and Figure 13 and TG curves are demonstrated in Figures 14-17. Moreover, the better thermal behavior of CNFs is reflected in the higher temperature of deterioration beginning. Irrespective of the source, when similar conditions (acid concentration, hydrolysis time, temperature) are used, it produces a similar result and shows the same trend. In the case of CNC, the surface area is smaller; hence, there is a small heat exposure area, which causes the degradation temperature to be low. Because of the greater heat contact area, tiny fiber parameters have a smaller breakdown temperature [12]. These short molecular chain lengths and flaw spots absorbed heat and began to break down at high temperatures, reducing NC's thermal [22].

### 3.5 Mechanical properties

Table 3 depicts the extraction method of nanocellulose from different sources and the effect on its mechanical properties. From Table 3, it can be seen that there has been an increase in the tensile strength to a great extent when nanocellulose is added to the composites. From the properties of the composite, after nanocellulose is added, the composites are more suitable for packaging industries.

<b>Table 3.</b> Extraction method of nanocellulose from different sources and the effect on its mechanical properties
---

Source	Method of extraction of nanocellulose		Length/Diameter fiber	Tensile strength	Elongation	Young's modulus	Water- vapor permeability	References	
Banana pseudo-	Alkali-urea solution with	PVA- 0.1 % NC added	100-500 nm	39.2 ± 1 MPa	122.1 ± 7 %	-	2.23 x 10 <sup>-10</sup> g m/m <sup>2</sup> d Pa	[31]	
stem ultrasonication	PVA- 0.5 % NC added		41.5 ± 1 MPa	129.1 ± 4 %	-	2.14 x 10 <sup>-10</sup> g m/m <sup>2</sup> d Pa			
		PVA-1 % NC added		42.6 ± 2 MPa	127.8 ± 8 %	-	2.07 x 10 <sup>-10</sup> g m/m <sup>2</sup> d Pa		
		PVA-3 % NC added		43.8 ± 4	139.5 ± 7 %	-	1.84 x 10 <sup>-10</sup> g m/m <sup>2</sup> d Pa		
		PVA-5 % NC added		28.7 ± 3	87.4 ± 5 %	-	1.14 x 10 <sup>-10</sup> g m/m <sup>2</sup> d Pa		
Banana peel	Enzymatic	CNF with 5% w/w containing 15 % peel bran	Length- $1490 \pm 107.3$ nm Diameter- $3.7 \pm 0.4$	96.6 ± 2.1 MPa	-	2064 ± 476.2 MPa	$6.4 \pm 0.4$	[4]	
		CNF with 5% w/w containing 35 % peel bran	Length- 1544.5 ± 40.6 nm Diameter- 8.8 ± 0.7 nm	65.5 ± 3.4 MPa	-	805.3 ± 77.5 MPa	16.6 ± 0.5		
Banana pseudo-	Acid hydrolysis	PVA with no NC	135.0 ± 12 nm	38.5 ± 3.6 MPa	61.0 ± 19.3 (%)	2522 ± 437	0.61 ± 0.04 g mm/kPa.h m <sup>2</sup>	[14]	
	with ultrasonication	PVA with 1% NC		42.1 ± 1.2 MPa	96.1 ± 7.6 (%)	2570 ± 146	0.56 ± 0.03 g mm/kPa.h m <sup>2</sup>		
		PVA with 3% NC		46.0 ± 2.7 MPa	74.3 ± 17.2 (%)	2940 ± 218	0.51 ± 0.03 g mm/kPa.h m <sup>2</sup>		
		PVA with 5% NC		35.4 ± 0.5 MPa	83.0 ± 12.5 (%)	2586 ± 74	0.44 ± 0.01 g mm/kPa.h m <sup>2</sup>		
Oil Palm	Chemical treatment	PLA with no NC)	-	54.7 ± 0.2 MPa	105.0 ± 0.3 %	933 ± 12 MPa	-	[32]	
biomass		PLA with 3 % NC	-	61.9 ± 0.9 MPa	105.0 ± 0 %	1280 ± 41 MPa	-		
		PLA with 5% NC	-	56.1 ± 0.5 MPa	106.0 ± 3 %	1067 ± 52 MPa	-		
	Chemical treatment	0% NC	-	26.1 ± 0.8 MPa	24.7 ± 1.2 %	741 4	2.50 ± 0.21 g mm cm/kPa.h cm <sup>2</sup>	[33]	
		0.5 % NC	-	4.6 ± 0.5 MPa	48.3 ± 1.2 %		2.55 ± 0.22 g mm cm/kPa.h cm <sup>2</sup>		
		1.0 % NC	-	11.2 ± 1.6 MPa	54.9 ± 4.2 %		2.27 ± 0.09g mm cm/kPa.h cm <sup>2</sup>	1	
Sugar palm	Chemical (H <sub>2</sub> SO <sub>4</sub>	Addition of 0.5% wt NC	Length 130 ± 30.23 nm	11.47 MPa	24.01 %	178.83 MPa	9.58 x 10 <sup>-10</sup> g/s.m.Pa	[15]	
	hydrolysis)	Addition of 1.0% wt NC	Diameter 5-6 nm	7.78 MPa	24.42 %	117.19 MPa			

For the banana composites, the elongation at break decreased with increased strength. One of the noticeable factors is that when the percentage of nanocellulose rises the water vapor permeability decreases along with decreased tensile strength. A similar trend was noticed in [31] and [32]. However, for the banana peel composite [4], the percentage increase of nanocellulose WVP also increased to 16.6 ± 0.5. This can be due to the percentage of banana bran used during the extraction of nanocellulose. Temperature, fiber content, orientation, permeability, surface protection, exposed surface area, and diffusivity all impact water absorption [15]. The barrier properties of the composites are also improved significantly. The mechanical properties nanocomposite material can be influenced by three aspects: (1) the nanofiller's dimensions and shape, (2) the processing method, and (3) the micro/nanostructure of the material, the interface for the matrix and the matrix/filler High aspect ratio nanofillers. Because of their large specific surface area, they were extremely intriguing, resulting in stronger reinforcing effects [15]. When nanocellulose is added to composites, there is a decrease in degradation temperature. It must be noted that the surface modification process while incorporating nanocellulose in the composite can also influence the tensile strength, Young's modulus, WVP, and strain.

Different sources of nanocellulose will have different surface modifications necessary to be added to the composite, and thus, the end performance will vary accordingly. Hence, a more comprehensive study must be done. Moreover, advanced computer-aided tools can be used to determine the properties of the composite reinforced with nanocellulose.

### 4. Conclusions

It can be concluded that nanocellulose has excellent potential in the food, semiconductor, biomedical, and biotechnology industries; it can successfully provide mechanical support to composites. In this review, chemical, mechanical, and a combination of both treatment methods have been discussed. Along with that, the effect of the type of treatment employed, the concentration of acid, hydrolysis time, ball milling, and sonicating power have been discussed. The diameter of cellulose nanocrystal and cellulose nanofiber are in the range of 4-80 nm despite the source and the treatment done; however, mechanical treatment will yield longer Fibers, and chemical treatment will yield shorter crystals. Thus, the aspect ratio will be affected accordingly. Higher yield will result in a higher crystalline index, and therefore, they show greater mechanical properties. Acid hydrolysis will lower the degradation temperature in the presence of the sulfate group. Nanocellulose extracted via mechanical treatment will show better thermal stability, but the treatment requires repeated/multiple cycles. Banana peel and pineapple leaf fiber showed the highest crystallinity with improved mechanical properties. Moreover, the composites filled with nanocellulose showed enhanced mechanical properties. The most suitable method of extraction is TEMPO-mediated oxidation combined with ultrasonication and high-pressure homogenization. However, nanocellulose extracted via TEMPO-mediated oxidation from sources like banana, pineapple, corn husk, sugar palm must be characterized using modern techniques like design expert software and small-scale implementations in different industries to understand the suitability of nanocellulose in biocomposites.

### Ethical issue

The authors are aware of and comply with best practices in publication ethics, specifically with regard to authorship (avoidance of guest authorship), dual submission, manipulation of figures, competing interests, and compliance with policies on research ethics. The authors adhere to publication requirements that the submitted work is original and has not been published elsewhere.

### Data availability statement

The manuscript contains all the data. However, more data will be available upon request from the authors.

### **Conflict of interest**

The authors declare no potential conflict of interest.

### References

- [1] Hu, D & Ma, W 2020, 'Nanocellulose as a Sustainable Building Block to Construct Eco-Friendly Thermally Conductive Composites', Industrial & Engineering Chemistry Research, vol. 59, no. 44, pp. 19465–19484.
- [2] Kim, J-H, Shim, BS, Kim, HS, Lee, Y-J, Min, S-K, Jang, D, Abas, Z& Kim, J 2015, 'Review of nanocellulose for sustainable future materials', International Journal of Precision Engineering and Manufacturing-Green Technology, vol. 2, no. 2, pp. 197–213.
- [3] Rajinipriya, M, Nagalakshmaiah, M, Robert, M & Elkoun, S 2018, 'Importance of Agricultural and Industrial Waste in the Field of Nanocellulose and Recent Industrial Developments of Wood Based Nanocellulose: A Review', ACS Sustainable Chemistry & Engineering, vol. 6, no. 3, American Chemical Society, pp. 2807–2828.
- [4] Tibolla, H, Pelissari, FM, Martins, JT, Lanzoni, EM, Vicente, AA, Menegalli, FC & Cunha, RL 2019, 'Banana starch nanocomposite with cellulose nanofibers isolated from banana peel by enzymatic treatment: In vitro cytotoxicity assessment', Carbohydrate Polymers, vol. 207, pp. 169–179.
- [5] Daud, Z, Hatta, MZM, Kassim, ASM, Awang, H & Aripin, AM 2013, Analysis the Chemical Composition and Fiber Morphology Structure of Corn Stalk, p. 5.
- [6] Jonoobi, M, Oladi, R, Davoudpour, Y, Oksman, K, Dufresne, A, Hamzeh, Y & Davoodi, R 2015, 'Different preparation methods and properties of nanostructured cellulose from various natural resources and residues: a review', Cellulose, vol. 22, no. 2, pp. 935–969

- [7] Tomoda, BT, Yassue-Cordeiro, PH, Ernesto, JV, Lopes, PS, Péres, LO, Silva, CF da & Moraes, MA de 2020, 'Chapter 3 Characterization of biopolymer membranes and films: Physicochemical, mechanical, barrier, and biological properties', in MA de Moraes, CF da Silva & RS Vieira (eds), Biopolymer Membranes and Films, Elsevier, pp. 67–95.
- [8] Ravindran, L, M.S, S & Thomas, S 2019, 'Novel processing parameters for the extraction of cellulose nanofibres (CNF) from environmentally benign pineapple leaf fibres (PALF): Structure-property relationships', International Journal of Biological Macromolecules, vol. 131, pp. 858–870.
- [9] Harini, K, Ramya, K & Sukumar, M 2018, 'Extraction of nano cellulose fibers from the banana peel and bract for production of acetyl and lauroyl cellulose', Carbohydrate Polymers, vol. 201, pp. 329–339.
- [10] Ferrante, A, Santulli, C & Summerscales, J 2020, 'Evaluation of Tensile Strength of Fibers Extracted from Banana Peels', Journal of Natural Fibers, vol. 17, no. 10, Taylor & Francis, pp. 1519–1531.
- [11] Pelissari, FM, Sobral, PJ do A & Menegalli, FC 2014, 'Isolation and characterization of cellulose nanofibers from banana peels', Cellulose, vol. 21, no. 1, pp. 417– 432
- [12] Faradilla, RHF, Lee, G, Rawal, A, Hutomo, T, Stenzel, MH & Arcot, J 2016, 'Nanocellulose characteristics from the inner and outer layer of banana pseudostem prepared by TEMPO-mediated oxidation', Cellulose, vol. 23, no. 5, pp. 3023–3037.
- [13] Khawas, P & Deka, SC 2016, 'Isolation and characterization of cellulose nanofibers from culinary banana peel using high-intensity ultrasonication combined with chemical treatment', Carbohydrate Polymers, vol. 137, pp. 608–616.
- [14] Pereira, ALS, Nascimento, DM do, Filho, M de sá MS, Morais, JPS, Vasconcelos, NF, Feitosa, JPA, Brígida, AIS & Rosa, M de F 2014, 'Improvement of polyvinyl alcohol properties by adding nanocrystalline cellulose isolated from banana pseudostems', Carbohydrate Polymers, vol. 112, pp. 165–172.
- [15] Ilyas, RA, Sapuan, SM, Ishak, MR & Zainudin, ES 2018, 'Development and characterization of sugar palm nanocrystalline cellulose reinforced sugar palm starch bionanocomposites', Carbohydrate Polymers, vol. 202, pp. 186–202.
- [16] Prado, KS & Spinacé, MAS 2019, 'Isolation and characterization of cellulose nanocrystals from pineapple crown waste and their potential uses', International Journal of Biological Macromolecules, vol. 122, pp. 410–416.
- [17] Cherian, BM, Leão, AL, Souza, SF de, Thomas, S, Pothan, LA & Kottaisamy, M 2010, 'Isolation of nanocellulose from pineapple leaf fibres by steam explosion', Carbohydrate Polymers, vol. 81, no. 3, pp. 720–725.
- [18] Mahardika, M, Abral, H, Kasim, A, Arief, S & Asrofi, M 2018, 'Production of Nanocellulose from Pineapple Leaf Fibers via High-Shear Homogenization and Ultrasonication', Fibers, vol. 6, no. 2.

- [19] Chen, D, Lawton, D, Thompson, MR & Liu, Q 2012, 'Biocomposites reinforced with cellulose nanocrystals derived from potato peel waste', Carbohydrate Polymers, vol. 90, no. 1, pp. 709–716.
- [20] Yang, X, Han, F, Xu, C, Jiang, S, Huang, L, Liu, L & Xia, Z 2017, 'Effects of preparation methods on the morphology and properties of nanocellulose (NC) extracted from corn husk', Industrial Crops and Products, vol. 109, pp. 241–247.
- [21] Rosa, MF, Medeiros, ES, Malmonge, JA, Gregorski, KS, Wood, DF, Mattoso, LHC, Glenn, G, Orts, WJ & Imam, SH 2010, 'Cellulose nanowhiskers from coconut husk fibers: Effect of preparation conditions on their thermal and morphological behavior', Carbohydrate Polymers, vol. 81, no. 1, pp. 83–92.
- [22] Liu, C, Li, B, Du, H, Lv, D, Zhang, Y, Yu, G, Mu, X & Peng, H 2016, 'Properties of nanocellulose isolated from corncob residue using sulfuric acid, formic acid, oxidative and mechanical methods', Carbohydrate Polymers, vol. 151, pp. 716–724.
- [23] Nang An, V, Chi Nhan, HT, Tap, TD, Van, TTT, Van Viet, P & Van Hieu, L 2020, 'Extraction of High Crystalline Nanocellulose from Biorenewable Sources of Vietnamese Agricultural Wastes', Journal of Polymers and the Environment, vol. 28, no. 5, pp. 1465–1474.
- [24] Soni, B, Hassan, EB & Mahmoud, B 2015, 'Chemical isolation and characterization of different cellulose nanofibers from cotton stalks', Carbohydrate Polymers, vol. 134, pp. 581–589.
- [25] Hassan, SH, Velayutham, TS, Chen, YW & Lee, HV 2021, 'TEMPO-oxidized nanocellulose films derived from coconut residues: Physicochemical, mechanical and electrical properties', International Journal of Biological Macromolecules, vol. 180, pp. 392–402.
- [26] Parikh, D, Thibodeaux, D & Condon, B 2007, 'X-ray Crystallinity of Bleached and Crosslinked Cottons', Textile Research Journal, vol. 77.
- [27] Lee, H-L, Chen, GC & Rowell, RM 2004, 'Thermal properties of wood reacted with a phosphorus pentoxide–amine system', Journal of Applied Polymer Science, vol. 91, no. 4, pp. 2465–2481.

- [28] Faria, LUS, Pacheco, BJS, Oliveira, GC & Silva, JL 2020, 'Production of cellulose nanocrystals from pineapple crown fibers through alkaline pretreatment and acid hydrolysis under different conditions', Journal of Materials Research and Technology, vol. 9, no. 6, pp. 12346–12353.
- [29] Lu, P & Hsieh, Y-L 2010, 'Preparation and properties of cellulose nanocrystals: Rods, spheres, and network', Carbohydrate Polymers, vol. 82, no. 2, pp. 329–336.
- [30] Jiang, F & Hsieh, Y-L 2013, 'Chemically and mechanically isolated nanocellulose and their self-assembled structures', Carbohydrate Polymers, vol. 95, no. 1, pp. 32–40.
- [31] Srivastava, KR, Dixit, S, Pal, DB, Mishra, PK, Srivastava, P, Srivastava, N, Hashem, A, Alqarawi, AA & Abd\_Allah, EF 2021, 'Effect of nanocellulose on mechanical and barrier properties of PVA-banana pseudostem fiber composite films', Environmental Technology & Innovation, vol. 21, p. 101312.
- [32] Ariffin, H, Norrrahim, MNF, Yasim-Anuar, TAT, Nishida, H, Hassan, MA, Ibrahim, NA & Yunus, WMZW 2018, 'Oil Palm Biomass Cellulose-Fabricated Polylactic Acid Composites for Packaging Applications', in M Jawaid & SK Swain (eds), Bionanocomposites for Packaging Applications, Springer International Publishing, Cham, pp. 95–105, viewed <a href="https://doi.org/10.1007/978-3-319-67319-65">https://doi.org/10.1007/978-3-319-67319-65</a>
- [33] Llanos, JHR & Tadini, CC 2018, 'Preparation and characterization of bio-nanocomposite films based on cassava starch or chitosan, reinforced with montmorillonite or bamboo nanofibers', International Journal of Biological Macromolecules, vol. 107, pp. 371–382.

This article is an open-access article distributed under the terms and conditions of the Creative Commons Attribution (CC BY) license (https://creativecommons.org/licenses/by/4.0/).